ACS APPLIED MATERIALS & INTERFACES

Research Article

www.acsami.org

Production of Centimeter-Scale Gradient Patterns by Graded Elastomeric Tip Array

Jin Wu and Jianmin Miao*

School of Mechanical and Aerospace Engineering, Nanyang Technological University, 50 Nanyang Avenue, Singapore 639798, Singapore

Supporting Information

ABSTRACT: Large-area patterned surfaces with chemical and/or morphological gradients have significant applications in biology, chemistry, and materials science. In this work, we developed a unique lithographic strategy to fabricate 2D and 3D gradient patterns with gradually varying feature size or height over centimeter-scale areas by utilizing a large-area polydimethylsiloxane (PDMS) tip array with programmable tip apex as a conformal photomask in near-field photolithography. Meanwhile, a new strategy was developed to create the PDMS tip array with graded apex size, which was employed to fabricate gradient patterns with the lateral feature sizes changing from sub-100 nm to several microns on one single substrate over macroscopic (square centimeter) areas. Furthermore, 3D gradient patterns with spatially varying feature height were enabled by employing gradient exposure dose. The formation of gradient feature size was ascribed either to gradient contact areas between tips and substrates or to exposure dose gradient. This lithography strategy combines the advantages of a wide range of feature sizes, simplicity, high-throughput, low-cost and diversified feature shapes, making it a facile and flexible approach to manufacture various functional gradient structures.

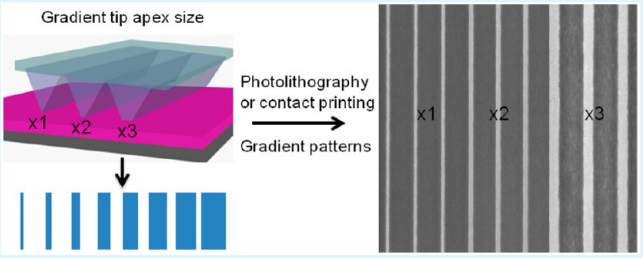

KEYWORDS: *gradient patterns, photolithography, PDMS tip array, elastomeric photomask, 3D structures*

INTRODUCTION

In recent years, patterns with tunable gradients of feature sizes, chemical, and physical properties[1−8] have drawn considerable attention owing to their variously significant applications ranging from biology and nanotechnology to materials science.[9−15] On the one hand, the gradient patterns could be utilized in fast and systematic screening of the behaviors of a large number of samples (e.g., cell adhesion).[10,16] On the other hand, the gradient patterns could also be employed for investigating dynamic phenomena such as the movement of water drops and cell migration and differentiation.[10,16−19] For example, patterns with gradually changing feature sizes spanning the nano- and microscale on one single substrate were recently used to probe important chemical and biological processes.[15,16,20,21] These patterns also open up the opportunity to study the statistic behaviors of a large population of samples with uniform experimental condition.[16] Besides 2D gradient patterns, 3D structures with spatially varying heights possess programmable surface area, mechanical compliance, and electromagnetic properties, which enable them to be used in various important applications, such as force sensing and light trapping.[1,2,17,22] For example, a library of polydimethylsiloxane (PDMS) elastomeric micropost array with spatially distributed mechanical compliances has been used to study the impacts of varying physical height on cell morphology, focal adhesion, and differentiation on one single substrate where the uniform biological environment is maintained.[1]

Although a large number of lithographic techniques, such as electron beam lithography (EBL),[23−25] UV-assisted capillary force lithography,[26] serial scanning-probe-based lithography (SPL),[27,28] and contact printing,[29,30] have been developed to fabricate patterns with gradient feature size or chemical composition, the production of patterns with tunable gradient feature sizes ranging from sub-100 nm to micrometer-length scales across centimeter-scale areas on one single substrate remains a challenge.[31,32] Recently, by tilting an elastomeric pyramidal pen array in the context of SPL,[16,28,33,34] combinatorial patterns with the dot sizes ranging from nano- to microscale have been realized, and the products of this enable a rapid and systematic screening of mesenchymal stem cell adhesion.[16,20] More recently, 3D polymer brushes have been fabricated in a massively parallel manner by controlling the spacing of nanofeatures based on an SPL platform.[35−38] Nevertheless, the production of gradient patterns by SPL strategies including polymer-pen lithography (PPL), beam-pen lithography (BPL) and dip-pen nanodisplacement lithography (DNL) demands an SPL platform and highly specific professional skills.[16,20,35,39−41] Thus, until now, the fabrication of 2D- and 3D-graded patterns with gradient lateral feature size and spatially varying feature height over centimeter-scale areas

Received: February 6, 2015
Accepted: March 12, 2015
Published: March 12, 2015

DOI: 10.1021/acsami.5b01158
ACS Appl. Mater. Interfaces 2015, 7, 6991−7000

in a simple and cost-effective manner is still challenging for state-of-the-art lithographic strategies.[10,42,43]

Photolithography is the major workhorse in the fabrication of micro/nanoscale structures over large areas owing to its highly parallel process, reliability, and well-established facilities and protocols.[11,44,45] However, there is difficulty with using this method in forming gradient patterns using conventional photomasks and photolithography. Previously, it was demonstrated that transparent PDMS reliefs could be used as photomasks to enable micro/nanostructures effectively because of their conformal merit, ease of use, and phase-shifting effect.[39,46,47] It was reported that the effective exposure doses at contact areas and at noncontact areas between transparent PDMS reliefs and underlying photoresist surface were different in near-field photolithography.[48,49] This difference could enable the selective exposure of the photoresist at contact areas while keeping the photoresist at noncontact regions underexposed.[42,45,48,49] Furthermore, it was also reported that the exposure dose could be adjusted to manipulate the size of the produced feature.[42,45] In state-of-the-art PDMS-structure-based lithographical strategies, the apex size of the PDMS relief is uniform across the whole tip array.[21,45,47] Hence, the patterns with uniform feature size are largely produced in these approaches, whether for microscale or nanoscale feature size.[48,50] Herein, we report the generation of combinatorial patterns with gradient feature size ranging from sub-100 nm to microscale over square centimeter areas on one single substrate by employing unmodified an elastomeric PDMS tip array as photomask. On the one hand, a novel avenue was developed to fabricate a silicon trench array and corresponding PDMS tip array with graded apex size. The PDMS tip array with gradient apex size was utilized to fabricate the aforementioned gradient patterns via photolithography. One the other hand, a PDMS tip array with uniform apex size was also employed to enable gradient patterns by exploiting near-field photolithography with the assistance of several different approaches, including applying gradient pressure between elastomeric photomask and substrate, oblique incident light exposure, and gradient exposure energy from the light source. Furthermore, 3D gradient polymer structures with spatially varying feature heights were fabricated via gradient exposure energy.

EXPERIMENTAL SECTION

Fabrication of Recessed Silicon Molds and Corresponding PDMS Tip Array. Shipley1805 (MicroChem) photoresist was spin-coated on Si/SiO_2 (100) wafers with a 280 nm thick SiO_2 layer to perform conventional photolithography on mask aligner (SUSS MJB4 UV400 from SUSS MicroTec company) using conventional Cr-coated hard photomasks. For generation of the recessed silicon trenches with gradient apex size at the bottom of the trenches, the conventional photomask with gradient microscale initial feature sizes 1, 2, 3, 4, and 6 μm on one single photomask was employed. For production of the recessed silicon trenches with uniform sub-100 nm apex size, the initial photomask with a uniform microscale feature size of 2 μm was utilized. After exposure and development of photoresist, the samples were put in buffered oxide etch (BOE, NH_4F/HF = 7:1, v/v, Transene Company) for 4 min to etch away the unprotected SiO_2 inside the photoresist features. After removal of photoresist from the sample surface by sonication in acetone, the samples were placed in KOH etching solution (30% KOH in H_2O/isopropanol (4:1 v/v)) at 75 °C to etch the exposed silicon features anisotropically, leading to the formation of recessed trench array with oblique sidewalls. For the initial feature sizes of 1, 2, 3, 4, and 6 μm on the same silicon substrate, the wet etching for 1.5 min produced the apex sizes of 30 ± 8 and 480 ± 33 nm and 1.3 ± 0.14, 2.5 ± 0.19, and 4.1 ± 0.32 μm at the bottom of silicon trenches, respectively. For the uniform initial feature size of 2 μm, the etching for 2 min produced the uniform apex size of 30 ± 8 nm at the bottom of trenches across the silicon trench array. After anisotropic etching, the remaining SiO_2 on the silicon mold was removed by putting samples in BOE. At last, the silicon molds were modified with 1H,1H,2H,2H-perfluorodecyltrichlorosilane (Gelest) by gas-phase silanization to facilitate the release of the PDMS structures from these molds.

Replication of PDMS Tip Array from the Molds. Hard/soft PDMS composites replicated from the silicon molds were utilized in near-field photolithography. The hard PDMS (h-PDMS) layer was composed of 3.4 g of vinyl-rich prepolymer (VDT-731, Gelest) and 1.0 g of hydrosilane-rich cross-linker (HMS-301). A 20 ppm w/w amount of platinum catalyst (platinumdivinyltetramethyldisiloxane complex in xylene, SIP 6831.1, Gelest) and 0.1% w/w modulator (2,4,6,8-tetramethyltetravinylcyclotetrasiloxane, Fluka) were required to add into the vinyl fraction for PDMS cross-linking. To prepare the soft PDMS (s-PDMS) mixture, the cross-linker and liquid PDMS elastomer (Sylgard 184, Dow Corning Singapore Pte. Ltd.) were mixed in a 1:10 ratio (w/w). The PDMS mixture was stirred and degassed. The h-PDMS mixture was spin-coated on the thus obtained silicon molds or photoresist-patterned molds and cured at 70 °C for 5 min. Subsequently, a liquid prepolymer layer of s-PDMS (3 mm) was poured onto the h-PDMS layer. After curing for 2 h, the hard/soft PDMS tip array was separated from the molds and used for photolithography.

Fabrication of Gradient Patterns Using PDMS Tip Array as Photomask in Photolithography. Shipley1805 (MicroChem) photoresist could be prediluted with propylene glycol monomethyl ether acetate (MicroChem). The Si/SiO_2 (100) wafers were spin coated with 20% (v/v) diluted photoresist and undiluted photoresist at 2500 rpm for 30 s to obtain 50 nm thick and 500 nm thick layers of photoresist, respectively. The photoresist-coated substrates were baked on a hot plate at 110 °C for 5 min before being used for photolithography. When the thus obtained PDMS tip array was placed on the photoresist-coated substrate surface manually, the van der Waals force brought PDMS in intimate and conformable contact with the underlying photoresist surface. A halogen light source (Fiber-lite Illuminators MI150, Dolan-Jenner) with Singale gooseneck BG2820 M with LH-759 lens was used to expose the photoresist through the PDMS photomask. Typically, the distance between the optical lens and underlying photoresist surface was 7 cm. The light with an exposure energy of 45 mw/cm^2 was used to expose the 50 nm thick photoresist at the contact areas between PDMS tip apexes and underlying substrate surfaces selectively. The typical exposure time was 10 s, and the development time was 15 s. Appropriate exposure dose was essential to ensure that the photoresist at the contact areas was selectively exposed because the increased exposure dose would make all photoresist be exposed completely. For production of the gradient patterns by applying nonuniform force, a force of 0.4 N was applied to one side of PDMS tip array, but no force was applied to the other side of the tip array during exposure. Specifically, after the PDMS tip array was placed in intimate contact with the photoresist-coated silicon wafers, a released-reverse (self-closing) tweezer (PELCO Reverse, Flat, TED PELLA, INC.) with a closing force of 0.4 N was employed to grip one side of PDMS tip array together with underlying silicon wafer but not the other side of the PDMS tip array. Therefore, the self-closing tweezer only applied pressure on one side of the PDMS array but not at the other side. After exposure, the self-closing tweezer was released and removed. For generation of gradient patterns using oblique light exposure, the incident light was illuminated with the angle of 45° relative to the vertical direction for exposure. To produce gradient patterns by making use of the exposure energy gradient resulting from light source, the distance between optical lens and underlying photoresist-coated surface was controlled to be 2 cm, and the exposure time was 2 s. The decreased distance between optical lens and photoresist surface not only enhanced the inhomogeneity of exposure energy because of the enlarged light spot size, but also increased the average exposure energy. For fabrication of 3D gradient patterns with varying feature height, a light with an exposure energy of

DOI: 10.1021/acsami.5b01158
ACS Appl. Mater. Interfaces 2015, 7, 6991−7000

250 mw/cm^2 was used to expose the 500 nm thick photoresist with an exposure time of 2 s. After photolithography, the photoresist patterns were evaporated with 12 nm Cr or 5 nm Cr/10 nm Au using electron beam evaporation, followed by photoresist liftoff in Remove PG (MicroChem Inc., USA) or acetone. Finally, the obtained gradient patterns were characterized using SEM (JEOL JSM-7600), AFM (Park Systems Co.) and optical microscopy (Olympus).

RESULTS AND DISCUSSION

In principle, if the PDMS tip array with a gradient of apex size ranging from nanoscale at one side to microscale at the other side is created, then it can be used to produce the patterns with a gradient feature size via near-field photolithography, because the apex sizes or contact areas between tip apex and underlying substrate surface define the size of the feature produced (Figure 1a).[28,48] In this work, by utilizing conventional photolithography followed by anisotropic wet etching, we developed a facile method to construct a recessed silicon trench array with the gradient apex size ranging from sub-100 nm to microscale on one single substrate (Figure S1 in Supporting Information). Hence, a PDMS graded tip array could be replicated from the obtained silicon mold and used for near-field photolithography.

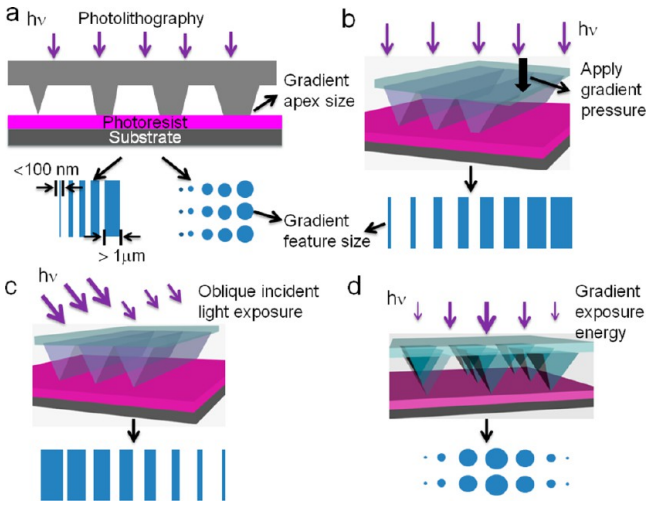

Figure 1. Schematic illustration of producing gradient patterns over centimeter-scale areas using PDMS tip array as photomask in near-field photolithography. (a) The PDMS tip array with graded apex size was utilized to produce patterns with gradient feature size increased gradually from less than 100 nm at the left side to microscale at the right side. (b) The external force was applied at one side of the PDMS tip array with uniform apex size but not applied at the other side during exposure, leading to the generation of gradient patterns. (c) The oblique incident light exposure brought about the exposure dose gradient, which led to the gradient feature size. (d) Utilization of graded exposure energy resulted from light source to produce gradient patterns.

For fabrication of the graded PDMS tip array, first, conventional Cr-based photomasks with gradient microscale feature sizes 1, 2, 3, 4, and 6 μm were utilized to generate gradient features in a 1:1 ratio on silicon wafer surface via conventional photolithography (Figure S1a,b in Supporting Information). Because the silicon anisotropic wet-etching speed in the vertical direction was the same, the large initial features required a longer etching time to get sharp apexes at the bottom of V-shape silicon trenches than did small initial features. Hence, by controlling the etching time, one side of the silicon wafer could be constructed with nanoscale apex size of 30 ± 8 nm, whereas the other side of the same wafer could be created with increased apex size up to 4.1 ± 0.32 μm (Figure 2a–d). Consequently, the PDMS tip array with corresponding gradient apex sizes changing from 60 ± 9 nm to 4.1 ± 0.31 μm could be replicated from the above obtained silicon mold (Figures 2e–h and S1e–f). By employing this gradient PDMS tip array as photomask in photolithography, the gradient photoresist patterns could be produced (Figure S2 in the Supporting Information). This was because the photoresist at contact areas between tips apexes and underlying photoresist could be selectively exposed completely, whereas the photoresist at noncontact areas was partially exposed (Figure S2c–d in the Supporting Information).[48] Therefore, after metal evaporation and photoresist liftoff, only the metals at the contacted areas were left. Hence, metal line patterns with gradient line width increasing from 80 ± 10 nm at one side (X coordinate = 0 mm) to 4.15 ± 0.32 μm at the other side (X coordinate = 6 mm) of the same substrate could be achieved (Figures 2i–l and 3n). Besides line patterns, a dot array with gradient spot size could also be achieved by utilizing a PDMS pyramidal tip array with gradient apex size as a photomask (Figure 3). The generated gradient dot size changed gradually from 80 ± 9 nm to 3.95 ± 0.24 μm across large areas (Figures 3i–l,n). It was found that both the PDMS tip apex size and correspondingly produced metal feature size increased monotonously with the increment of initial feature size on conventional Cr-based photomasks (Figure 3m). Furthermore, the produced feature shapes were the same as the PDMS tip apex shapes for all the feature shapes explored here, including straight line, stripe, dot, and square (Figures 2 and 3), demonstrating that the photoresist at contacted areas was selectively exposed.

In addition to the delivery of energy in photolithography, PDMS-based micro/nanostructures have also been widely used as powerful tools to deliver materials directly on substrates for construction of micro/nanostructures, as in the cases of soft lithography and molecular printing.[51−53] For example, by controlling the amount of metal ions in the block copolymer matrix, scanning probe block copolymer lithography enables the synthesis and position of sub-10 nm individual nanoparticles in large areas in situ.[41] In these strategies, the size of contact region between the PDMS tip apex and substrate surface is the key to define produced feature size because the materials are selectively delivered to substrate surface at these regions. Herein, the PDMS tip array with a gradient of apex size was successfully utilized to fabricate the patterns with gradient feature size ranging from sub-100 nm to several microns over centimeter-scale areas via contact printing (Figures S3 and S4 in the Supporting Information). This strategy could be employed to fabricate the smallest silver dot size of 51 ± 7 nm (Figure S3g in the Supporting Information). In contrast, the produced feature size was homogeneous when the PDMS tip array with uniform apex size was utilized in contact printing (Figure S5 in the Supporting Information). Variously shaped patterns were enabled in this manner. It demonstrated that the PDMS tip array with gradient apex size could be utilized to define materials with gradient feature size via different lithographic strategies.

Recently, the pressure between elastomeric PDMS tip array and underlying sample surface has been expolited as a significant tool to control the feature size and reaction rate in the context of SPL.[33,34,40,54,55] In this study, besides the PDMS tips with gradient apex size, the PDMS tip array with uniform

DOI: 10.1021/acsami.5b01158
ACS Appl. Mater. Interfaces 2015, 7, 6991−7000

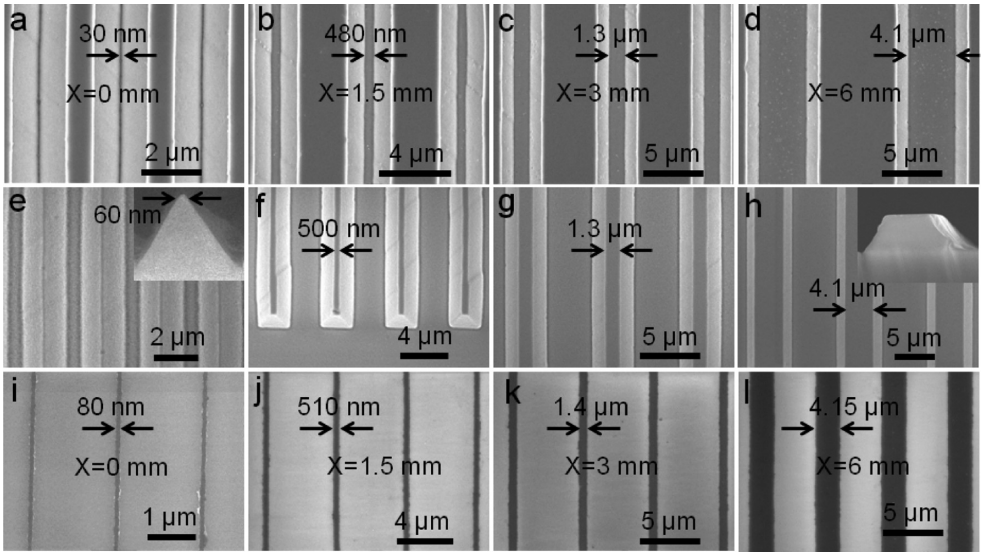

Figure 2. Fabrication of gradient line patterns by employing PDMS tip array with gradient apex size as photomask in photolithography. (a, b, c, and d) SEM images of silicon trenches with the apexes sizes of 30 ± 8 nm, 480 ± 33 nm, 1.3 ± 0.14 μm, and 4.1 ± 0.32 μm respectively, which were located at the positions with X coordinates of 0, 1.5, 3, and 6 mm, respectively, on the same substrate. The above silicon trenches were fabricated from initial patterns with the feature sizes of 1, 2, 3, and 6 μm, respectively, on conventional Cr-based photomask. (e, f, g, and h) SEM images of PDMS tips with the apexes sizes of 60 ± 9 nm, 500 ± 35 nm, 1.3 ± 0.11 μm, and 4.1 ± 0.31 μm, respectively, which were replicated from the silicon trenches in a, b, c, and d, respectively. (i, j, k, and l) SEM images of Cr lines with the line widths of 80 ± 10 nm, 510 ± 39 nm, 1.4 ± 0.14 μm, and 4.15 ± 0.32 μm, respectively, which were fabricated by using the PDMS tips in e, f, g, and h, respectively.

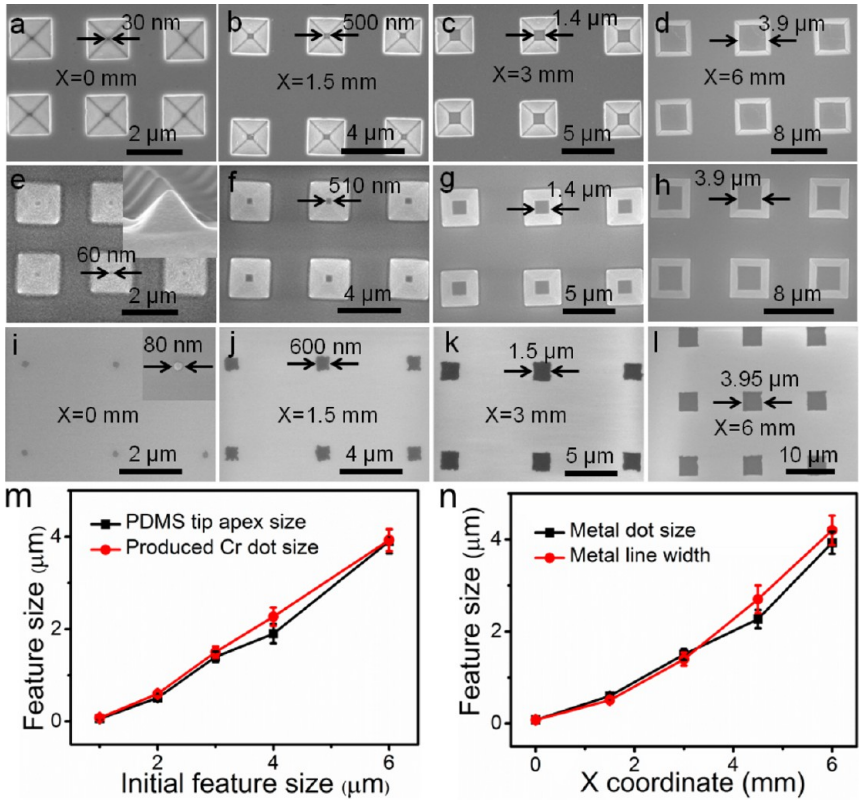

Figure 3. Fabrication of gradient dot patterns by employing PDMS pyramidal tip array with gradient apex size. (a, b, c, and d) SEM images of the recessed silicon pyramids with the apex sizes of 30 ± 8 nm, 500 ± 35 nm, 1.4 ± 0.12 μm, and 3.9 ± 0.22 μm, respectively, which were located at the positions with X coordinates of 0, 1.5, 3, and 6 mm, respectively. (e, f, g, and h) SEM images of PDMS pyramidal tips with the apexes sizes of 60 ± 9 nm, 510 ± 45 nm, 1.4 ± 0.11 μm, and 3.9 ± 0.26 μm, respectively, which were replicated from the silicon pyramids in a, b, c, and d, respectively. (i, j, k, and l) SEM images of Cr dot arrays with the edge lengths of 80 ± 9 nm, 600 ± 55 nm, 1.5 ± 0.12 μm, and 3.95 ± 0.24 μm, respectively, which were made by the PDMS tips in e, f, g, and h, respectively. (m) Plot of PDMS tip apex size and correspondingly produced Cr dot size as a function of the initial feature size on conventional photomask. (n) Plot of produced metal dot size and line width of gradient patterns as a function of X coordinates on substrate.

DOI: 10.1021/acsami.5b01158
ACS Appl. Mater. Interfaces 2015, 7, 6991−7000

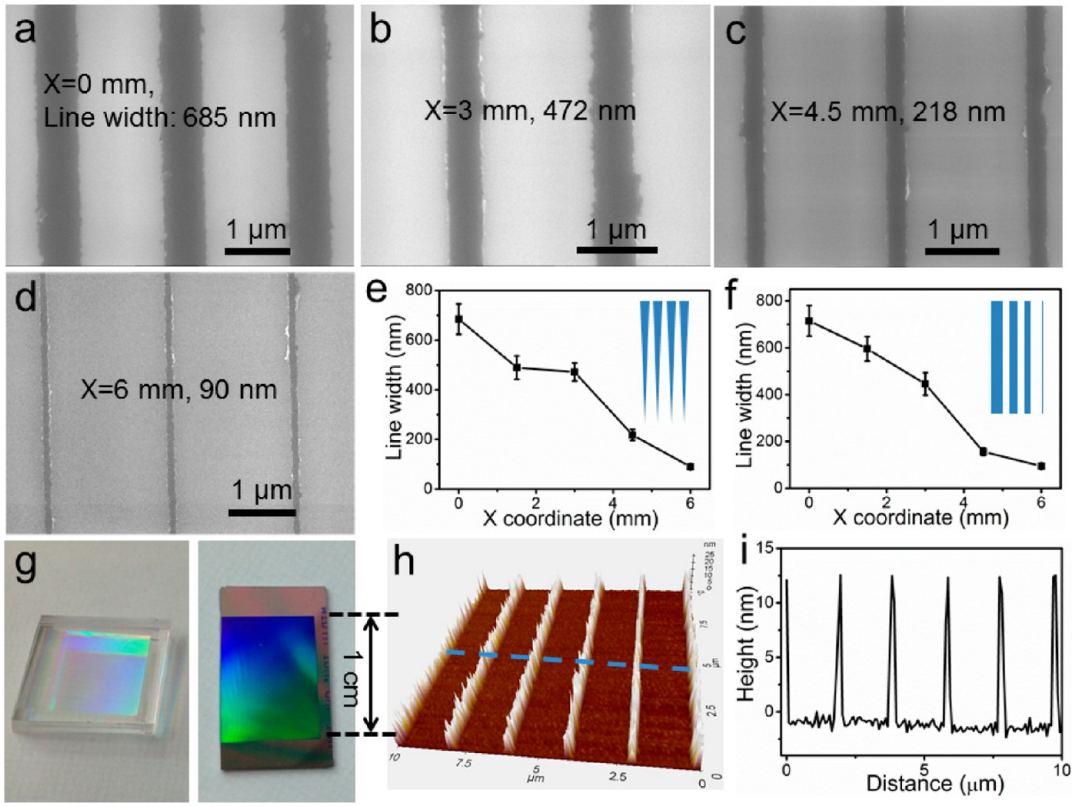

Figure 4. Creation of gradient patterns by applying nonuniform force on two sides of elastomeric photomask. (a, b, c, and d) SEM images of Cr line segments with the line widths of 685 ± 60, 472 ± 36, 218 ± 22, and 90 ± 10 nm, respectively, which were located at the positions with X coordinates of 0, 3, 4.5, and 6 mm, respectively, on substrate. (e) The Cr line widths changed as a function of X coordinates from one end to the other end of the same lines. (f) The Cr line widths changed as a function of X coordinates from one side to the other side of the substrate for different lines. (e and f, insets) Gradient line width change directions. (g) Optical images of centimeter-scale elastomeric photomask, left, and correspondingly produced gradient patterns, right. (h) 3D AFM topographical image of the Cr lines in d. (i) AFM height profile of the blue line across the patterns in h indicating of the uniform height of 12 ± 0.9 nm for the Cr patterns.

apex size could also be employed to generate gradient patterns by applying nonuniform pressure on the backside of elastomeric photomasks during exposure (Figure 4). Specifically, the external force was applied at one side of elastomeric photomask, but no force was applied at the other side. Because of the elastic nature of PDMS, the external force led to the deformation of tips beneath the force applied position.[23,35] Thereby the contact areas enlarged at these regions. As the other side of the PDMS photomask was free of force, the deformation of tips decreased gradually from the force-applied side to the other, force-free side, and so did the contact areas. Consequently, the gradient patterns with the line width changed from 685 ± 60 nm at the force-applied side to 90 ± 10 nm at the other, force-free side of substrate were generated (Figure 4a–e). Because the periodicity of all patterns was the same (2 μm), the above gradient patterns also exhibited gradient spacing changing from 1.3 ± 0.12 μm at one side to 1.9 ± 0.02 μm at the other side (Figure 4a–d). Besides the gradient patterns with varied line width from one end to the other end for the same lines, the gradient patterns with line width changed from one line to other lines could also be obtained by changing the external force-applied position (Figure 4e–f). Noticeably, both the centimeter-scale soft photomask and fabricated gradient patterns displayed diffraction color (Figure 4g), indicating of an ordered distribution of surface textures over the soft mask surface as well as the obtained gradient patterns. The atomic force microscopy (AFM) topographical image demonstrated that the fabricated Cr patterns had an average height of 12 ± 0.9 nm (Figure 4h–i).

Besides utilization of gradient contact areas to fabricate graded patterns as explored above, exposure dose gradient can also be exploited to enable gradient patterns using the transparent PDMS tip array with uniform apex size as photomask in near-field photolithography (Figure 1c,d). This is because the increased exposure dose leads to the increment of feature size.[28] Consequently, herein we explored the fabrication of gradient patterns by utilizing oblique incident light for exposure (Figures 1c and 5). In the case of exposure with oblique incident light, the side of photomask near the light source received larger exposure dose than the other side far away from the light source did, leading to the formation of exposure dose gradient distribution across the photomask. Consequently, the generated Au dot size decreased monotonously from the side near the light source to the other side far away from the light source on substrate (Figure 5a–f). Besides the feature shapes of dot and line, gradient patterns with other feature shapes could also be enabled by utilizing the correspondingly shaped PDMS tip array as photomask. For example, by making use of the PDMS grid tip array in this lithographic fashion, the metal grid patterns with gradient line width from 675 ± 59 to 110 ± 11 nm could be produced (Figure 5h–l). Additionally, with the straight PDMS tip array as photomask, the patterns with gradually changed line width

DOI: 10.1021/acsami.5b01158
ACS Appl. Mater. Interfaces 2015, 7, 6991–7000

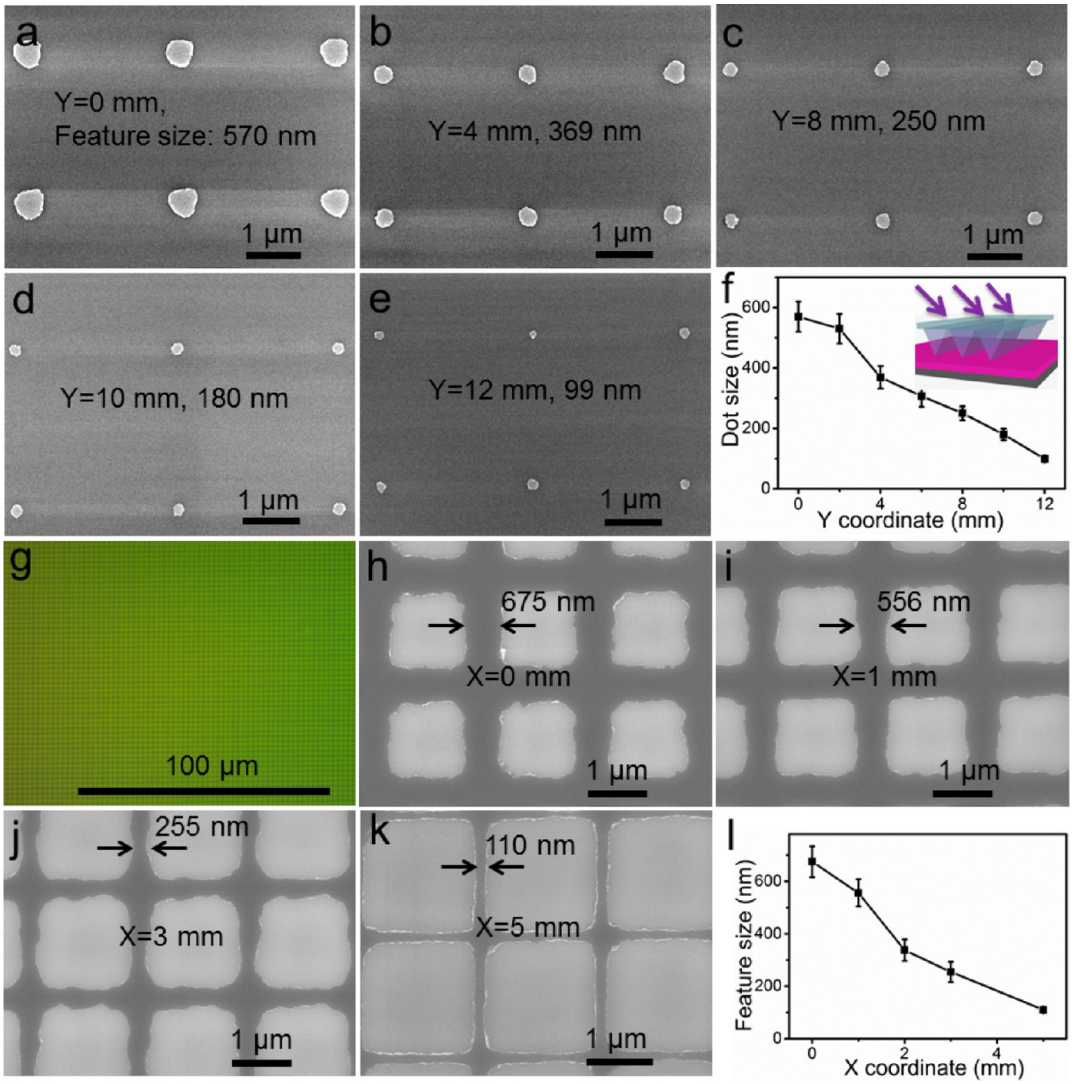

Figure 5. Construction of gradient metal patterns using oblique incident light for exposure through PDMS photomasks. (a, b, c, d, and e) SEM images of gold dot array with the feature sizes of 570 ± 50, 369 ± 37, 250 ± 23, 180 ± 19, and 99 ± 10 nm, respectively, which were positioned from the left side to the right side of substrate with Y coordinates of 0, 4, 8, 10, and 12 mm, respectively. (f) Plot of the gold dot size as a function of Y coordinates. (g) Large-area optical image of grid photoresist patterns with subwavelength line width. (h, i, j, and k) SEM images of Cr grid patterns with gradient line widths of 675 ± 59, 556 ± 52, 255 ± 39, and 110 ± 11 nm, respectively, which were positioned at the locations with the X coordinates of 0, 1, 3, and 5 mm, respectively. (l) Plot of the produced Cr line width as a function of X coordinates.

were also enabled in this manner (Figure S6 in the Supporting Information). In principle, this lithography methodology could also allow for the production of gradient patterns with other diversified shapes by exploiting the PDMS tips with corresponding shapes as photomasks.

In addition to the oblique light exposure induced exposure dose gradient, the nonuniform exposure energy from point light source could also lead to an exposure dose gradient across the substrate surface (Figures 1d and 6). The exposure energy of incident light from the lens of the halogen light source used here was not absolutely homogeneous within the light spot. The exposure energy in the center of light spot was the highest, and that in the surrounding areas was the lowest. Hence, the photoresist below the central part of PDMS photomasks received a larger effective exposure dose than that in surrounding areas did. As a result, the obtained gradient patterns had the largest photoresist dot size of 508 ± 45 nm in the center of substrate (X coordinate = 8 mm) and the smallest dot size of 95 ± 10 nm at the edge of substrate (X coordinate = 0 mm, Figure 6a–f). Likewise, the gradient line patterns were also constructed with the largest line width of 534 ± 57 nm in the center and the smallest line width of 180 ± 21 nm in the surrounding areas of substrate (Figure 6g–l). Furthermore, the obtained gradient photoresist patterns could be transferred into silicon to fabricate the pyramidal silicon molds with gradient apex size (Figure S7a–e in the Supporting Information). The apex sizes of fabricated gradient silicon molds increased from the edge to the center, and then decreased from the center to the other edge. Consequently, the corresponding PDMS pyramidal tip array with gradient apex size could be replicated from the above silicon molds and could be employed as the second-generation photomask to fabricate gradient patterns in near-field photolithography (Figure S7f–m in the Supporting Information). It demonstrated that the PDMS tip array with gradient apex size and correspondingly fabricated gradient patterns were transferable between each other.

Near-field photolithography using the PDMS tip array with gradient exposure energy not only enables gradient lateral

DOI: 10.1021/acsami.5b01158
ACS Appl. Mater. Interfaces 2015, 7, 6991–7000

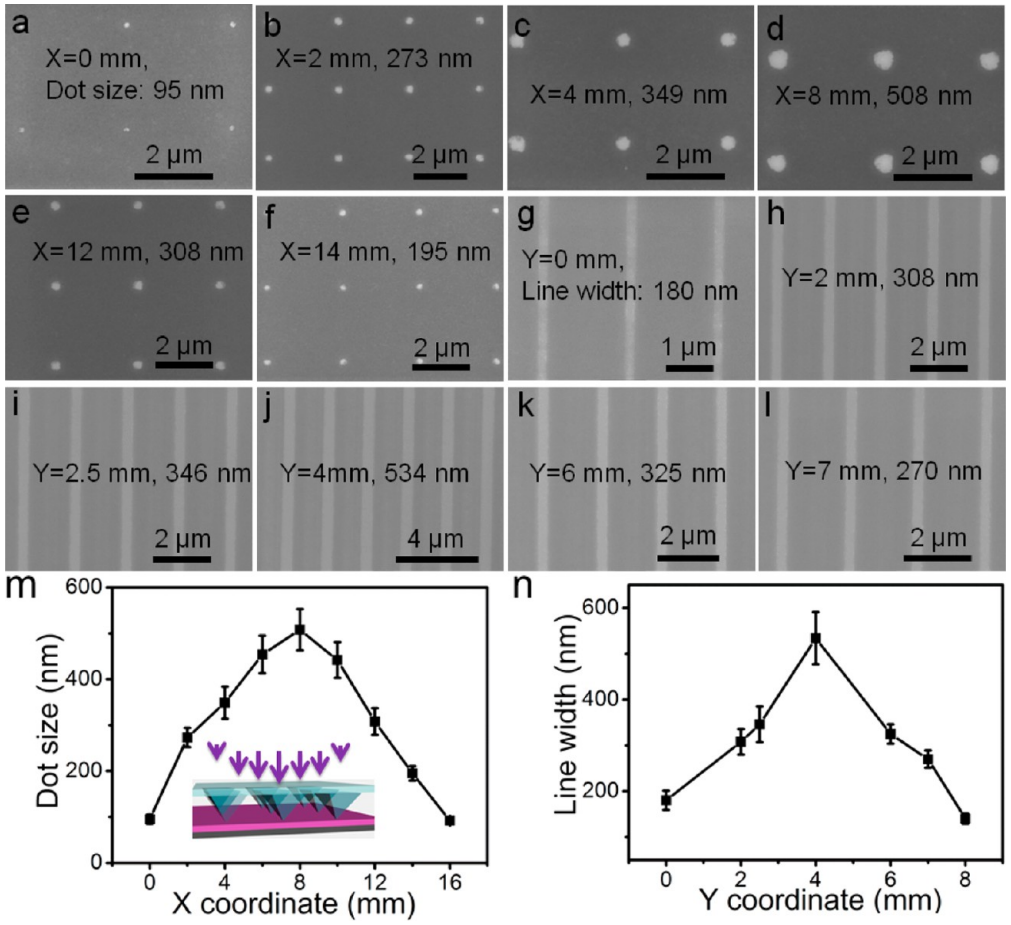

Figure 6. Production of gradient patterns by employing gradient exposure energy resulted from light source in photolithography. (a, b, c, d, e, and f) SEM images of positive photoresist dot arrays with the spot sizes of 95 ± 10, 273 ± 21, 349 ± 35, 508 ± 45, 308 ± 29, and 195 ± 16 nm, respectively, which were located at the positions with X coordinates of 0, 2, 4, 8, 12, and 14 mm, respectively, on substrate. (g, h, i, j, k, and l) SEM images of positive photoresist line patterns with gradient line widths of 180 ± 21, 308 ± 28, 346 ± 39, 534 ± 57, 325 ± 21, and 270 ± 19 nm, respectively, which were at the positions with Y coordinates of 0, 2, 2.5, 4, 6, and 7 mm, respectively. (m) Plot of the obtained photoresist dot size as a function of X coordinate. Inset, schematic illustrating the experimental condition. (n) Plot of the obtained photoresist line width as a function of Y coordinate.

feature sizes as explored above but also realizes 3D gradient structures with spatially varying feature height (Figure 7). In this study, it was found that the incident light would make the photoresist underexposed when a thick positive photoresist layer (such as 500 nm thick used here) and low exposure dose (such as the exposure time of 2 s used here) were utilized. Consequently, the positive photoresist at exposed areas was partially removed after development, and therefore, nanoscale photoresist trenches formed on the substrate. As mentioned above, the nonuniform exposure energy resulting from the point light source makes the center of substrate surface receive larger exposure dose than the edges of the substrate do. Consequently, the obtained recessed photoresist trenches in the center were deeper than those at the edges, leading to the formation of recessed trench patterns with gradient depth (Figure 7b,c). For example, the positive photoresist trenches with the depths of 100 ± 11, 160 ± 18, and 240 ± 21 nm were produced at the edge (X coordinate = 0 mm), near the edge (X coordinate = 4 mm), and in the center of the substrate surface (X coordinate = 8 mm) respectively. Hence, the PDMS relief or pillar array with spatially varying height could be replicated by employing these photoresist patterns as molds (Figure 7d–f). For instance, the raised PDMS reliefs with gradient heights changed gradually from 100 ± 12 nm at the edge (X coordinate = 0 mm) to 160 ± 20 nm near the edge (X coordinate = 4 mm) and 240 ± 25 nm in the center of the PDMS reliefs (X coordinate = 8 mm, Figure 7d–f).

In previously reported SPL studies, the spacing between features can be made as small as a few nanometer because the tips were mounted onto high-resolution piezoactuators.[56] Nevertheless, the costly scanning probe platform is required for SPL, such as PPL and BPL. In comparison with the fabrication of large-area 2D and 3D gradient structures based on an SPL platform,[16,28,35−38] the lithographic strategy developed here bypasses the requirement of a scanning probe platform, making it not only simple and cost-effective but also reliable. However, the shortcoming of this strategy is the low density of structures achieved on surfaces because their pitch is determined by the original chrome photomask. In future work, the density of produced structures could be increased by utilizing other lithographical means instead of conventional photolithography to fabricate the silicon molds with small feature periodicity, such as EBL and nanoimprint lithography.[23,25,57]

DOI: 10.1021/acsami.5b01158
ACS Appl. Mater. Interfaces 2015, 7, 6991−7000

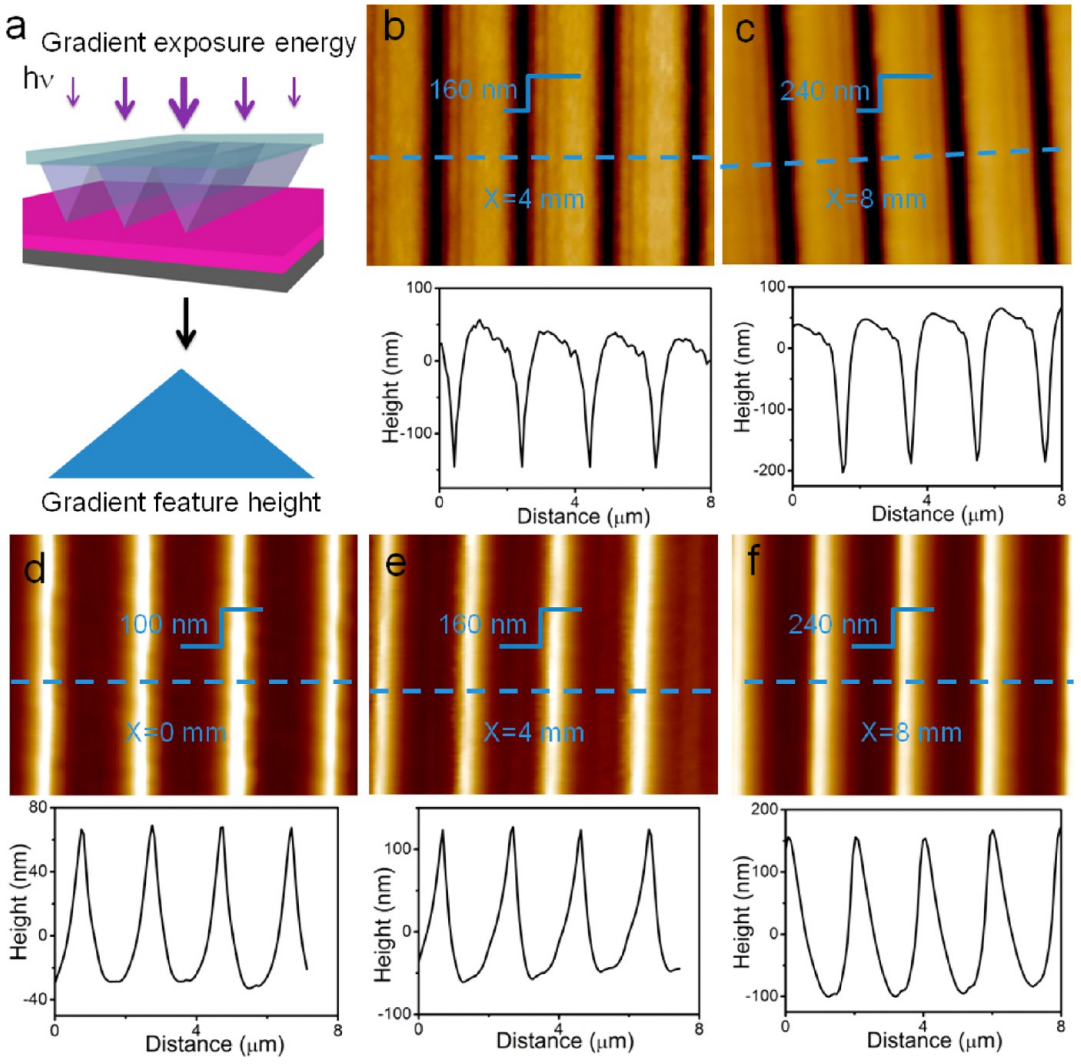

Figure 7. Fabrication of 3D structures with spatially varying feature height. (a) Scheme illustrating the fabrication of patterns with gradient feature height using exposure energy gradient. (b and c) AFM topographical images of recessed positive photoresist trenches with the depths of 160 ± 18 and 240 ± 21 nm, respectively, which were located near the edge (X = 4 mm) and in the center (X = 8 mm) of substrate. (d, e, and f) AFM topographical images of PDMS reliefs with the heights of 100 ± 12, 160 ± 20, and 240 ± 25 nm, respectively, which were located at the positions with X coordinates of 0, 4, and 8 mm, respectively. The PDMS reliefs in e and f were replicated from the photoresist trenches in b and c, respectively.

CONCLUSIONS

We developed several lithographic methods to fabricate the patterns with gradient feature size ranging from sub-100 nm to microscale over centimeter-scale areas by utilizing a PDMS tip array as a photomask in near-field photolithography. For the first time, we fabricated a V-shape PDMS tip array with gradient apex size by using simple silicon anisotropic etching and utilized such tips to create gradient patterns in a facile, scalable, and reliable manner. Besides 2D gradient patterns, large-area 3D gradient patterns with spatially varying feature height were also enabled. The formation of gradient patterns was attributed to either the gradient contact areas between tip apexes and substrate or exposure dose gradient. Importantly, the feature shapes of gradient patterns were not limited to dot, but also could be extended to many other shapes, such as continuous line and grid. Note that the patterns characteristics such as the smallest achievable feature size and uniformity could be programmed using different materials to make the elastomeric arrays in the context of this reported printing method in future work.[58,59] This technique can be easily handled and accessed to fabricate various gradient structures, so it could be optimized in the future as a generalized micro/nanofabrication approach. It is envisioned that this lithographic approach can be employed to fabricate patterns of other gradients such as biochemical gradients for a variety of biological studies (e.g., stem cells adhesion and differentiation, tissue engineering, and cancer cell metastasis).[5,28,60−62]

ASSOCIATED CONTENT

Supporting Information

Schemes illustrating the steps of fabricating PDMS tip arrays with gradient and uniform apex sizes respectively, 3D AFM topographical images of PDMS tip array and correspondingly produced photoresist patterns, the fabrication of gradient patterns and uniform patterns with various shapes via contact printing, the fabrication of gradient metal line patterns by utilizing oblique incident light for exposure, and the generation of silicon molds with gradient apex size using PDMS pyramidal photomask with gradient apex size. This material is available free of charge via the Internet at http://pubs.acs.org.

DOI: 10.1021/acsami.5b01158
ACS Appl. Mater. Interfaces 2015, 7, 6991−7000

AUTHOR INFORMATION

Corresponding Author

*E-mail: MJMMiao@ntu.edu.sg.

Notes

The authors declare no competing financial interest.

REFERENCES

(1) Fu, J. P.; Wang, Y. K.; Yang, M. T.; Desai, R. A.; Yu, X. A.; Liu, Z. J.; Chen, C. S. Mechanical Regulation of Cell Function with Geometrically Modulated Elastomeric Substrates. *Nat. Methods* **2010**, *7*, 733−736.

(2) Vogel, V.; Sheetz, M. Local Force and Geometry Sensing Regulate Cell Functions. *Nat. Rev. Mol. Cell Biol.* **2006**, *7*, 265−275.

(3) Koo, H. J.; Waynant, K. V.; Zhang, C.; Braun, P. V. Polymer Brushes Patterned with Micrometer-Scale Chemical Gradients Using Laminar Co-Flow. *ACS Appl. Mater. Interfaces* **2014**, *6*, 14320−14326.

(4) Shi, J.; Wang, L.; Zhang, F.; Li, H.; Lei, L.; Liu, L.; Chen, Y. Incorporating Protein Gradient into Electrospun Nanofibers as Scaffolds for Tissue Engineering. *ACS Appl. Mater. Interfaces* **2010**, *2*, 1025−1030.

(5) Wu, J.; Zan, X. L.; Li, S. Z.; Liu, Y. Y.; Cui, C. L.; Zou, B. H.; Zhang, W. N.; Xu, H. B.; Duan, H. W.; Tian, D. B.; Huang, W.; Huo, F. W. In Situ Synthesis of Large-Area Single Sub-10 nm Nanoparticle Arrays by Polymer Pen Lithography. *Nanoscale* **2014**, *6*, 749−752.

(6) Faustini, M.; Ceratti, D. R.; Louis, B.; Boudot, M.; Albouy, P. A.; Boissiere, C.; Grosso, D. Engineering Functionality Gradients by Dip Coating Process in Acceleration Mode. *ACS Appl. Mater. Interfaces* **2014**, *6*, 17102−17110.

(7) Zhang, G. Y.; Zhang, X.; Li, M.; Su, Z. H. A Surface with Superoleophilic-to-Superoleophobic Wettability Gradient. *ACS Appl. Mater. Interfaces* **2014**, *6*, 1729−1733.

(8) Hale, N. A.; Yang, Y.; Rajagopalan, P. Cell Migration at the Interface of A Dual Chemical- Mechanical Gradient. *ACS Appl. Mater. Interfaces* **2010**, *2*, 2317−2324.

(9) Karuturi, S. K.; Liu, L.; Su, L. T.; Chutinan, A.; Kherani, N. P.; Chan, T. K.; Osipowicz, T.; Yoong Tok, A. I. Gradient Inverse Opal Photonic Crystals via Spatially Controlled Template Replication of Self-Assembled Opals. *Nanoscale* **2011**, *3*, 4951−4954.

(10) Genzer, J.; Bhat, R. R. Surface-Bound Soft Matter Gradients. *Langmuir* **2008**, *24*, 2294−2317.

(11) Wu, J.; Yu, C. H.; Li, S. Z.; Zou, B. H.; Liu, Y. Y.; Zhu, X. Q.; Guo, Y. Y.; Xu, H. B.; Zhang, W. N.; Zhang, L. P.; Liu, B.; Tian, D. B.; Huang, W.; Sheetz, M. P.; Huo, F. W. Parallel Near-Field Photolithography with Metal-Coated Elastomeric Masks. *Langmuir* **2015**, *31*, 1210−1217.

(12) Chen, T.; Amin, I.; Jordan, R. Patterned Polymer Brushes. *Chem. Soc. Rev.* **2012**, *41*, 3280−3296.

(13) Lin, X. K.; He, Q.; Li, J. B. Complex Polymer Brush Gradients Based on Nanolithography and Surface-Initiated Polymerization. *Chem. Soc. Rev.* **2012**, *41*, 3584−3593.

(14) Ratner, B. D.; Bryant, S. J. Biomaterials: Where We Have Been and Where We Are Going. *Annu. Rev. Biomed. Eng.* **2004**, *6*, 41−75.

(15) Morgenthaler, S.; Zink, C.; Spencer, N. D. Surface-Chemical and -Morphological Gradients. *Soft Matter* **2008**, *4*, 419−434.

(16) Giam, L. R.; Massich, M. D.; Hao, L. L.; Wong, L. S.; Mader, C. C.; Mirkin, C. A. Scanning Probe-Enabled Nanocombinatorics Define the Relationship between Fibronectin Feature Size and Stem Cell Fate. *Proc. Natl. Acad. Sci. U.S.A.* **2012**, *109*, 4377−4382.

(17) Li, X. M.; Tian, H. M.; Shao, J. Y.; Ding, Y. C.; Liu, H. Z. Electrically Modulated Microtransfer Molding for Fabrication of Micropillar Arrays with Spatially Varying Heights. *Langmuir* **2013**, *29*, 1351−1355.

(18) Sommers, A. D.; Brest, T. J.; Eid, K. F. Topography-Based Surface Tension Gradients to Facilitate Water Droplet Movement on Laser-Etched Copper Substrates. *Langmuir* **2013**, *29*, 12043−12050.

(19) Chaudhury, M. K.; Whitesides, G. M. How to Make Water Run Uphill. *Science* **1992**, *256*, 1539−1541.

(20) Cabezas, M. D.; Eichelsdoerfer, D. J.; Brown, K. A.; Mrksich, M.; Mirkin, C. A. Combinatorial Screening of Mesenchymal Stem Cell Adhesion and Differentiation Using Polymer Pen Lithography. *Methods Cell Biol.* **2014**, *119*, 261−276.

(21) Eichelsdoerfer, D. J.; Liao, X.; Cabezas, M. D.; Morris, W.; Radha, B.; Brown, K. A.; Giam, L. R.; Braunschweig, A. B.; Mirkin, C. A. Large-Area Molecular Patterning with Polymer Pen Lithography. *Nat. Protoc.* **2013**, *8*, 2548−2560.

(22) Discher, D. E.; Janmey, P.; Wang, Y. L. Tissue Cells Feel and Respond to the Stiffness of Their Substrate. *Science* **2005**, *310*, 1139−1143.

(23) Turchanin, A.; Tinazli, A.; El-Desawy, M.; Großmann, H.; Schnietz, M.; Solak, H. H.; Tampé, R.; Gölzhäuser, A. Molecular Self-Assembly, Chemical Lithography, and Biochemical Tweezers: A Path for the Fabrication of Functional Nanometer-Scale Protein Arrays. *Adv. Mater.* **2008**, *20*, 471−477.

(24) Ballav, N.; Chen, C. H.; Zharnikov, M. Electron Beam and Soft X-ray Lithography with A Monomolecular Resist. *J. Photopolym. Sci. Technol.* **2008**, *21*, 511−517.

(25) Gölzhäuser, A.; Geyer, W.; Stadler, V.; Eck, W.; Grunze, M.; Edinger, K.; Weimann, T.; Hinze, P. Nanoscale Patterning of Self-Assembled Monolayers with Electrons. *J. Vac. Sci. Technol., B* **2000**, *18*, 3414−3418.

(26) Kim, D.-H.; Seo, C.-H.; Han, K.; Kwon, K. W.; Levchenko, A.; Suh, K.-Y. Guided Cell Migration on Microtextured Substrates with Variable Local Density and Anisotropy. *Adv. Funct. Mater.* **2009**, *19*, 1579−1586.

(27) Liu, X. Q.; Li, Y.; Zheng, Z. J. Programming Nanostructures of Polymer Brushes by Dip-Pen Nanodisplacement Lithography (DNL). *Nanoscale* **2010**, *2*, 2614−2618.

(28) Zhou, Y.; Xie, Z.; Brown, K. A.; Park, D. J.; Zhou, X. Z.; Chen, P. C.; Hirtz, M.; Lin, Q. Y.; Dravid, V. P.; Schatz, G. C.; Zheng, Z. J.; Mirkin, C. A. Apertureless Cantilever-Free Pen Arrays for Scanning Photochemical Printing. *Small* **2014**, *11*, 913−918.

(29) Larsson, A.; Liedberg, B. Poly(ethylene glycol) Gradient for Biochip Development. *Langmuir* **2007**, *23*, 11319−11325.

(30) Choi, S. H.; Newby, B. M. Z. Micrometer-Scaled Gradient Surfaces Generated Using Contact Printing of Octadecyltrichlorosilane. *Langmuir* **2003**, *19*, 7427−7435.

(31) Ballav, N.; Schilp, S.; Zharnikov, M. Electron-Beam Chemical Lithography with Aliphatic Self-Assembled Monolayers. *Angew. Chem., Int. Ed.* **2008**, *47*, 1421−1424.

(32) Schilp, S.; Ballav, N.; Zharnikov, M. Fabrication of A Full-Coverage Polymer Nanobrush on An Electron-Beam-Activated Template. *Angew. Chem., Int. Ed.* **2008**, *47*, 6786−6789.

(33) Liao, X.; Braunschweig, A. B.; Mirkin, C. A. "Force-Feedback" Leveling of Massively Parallel Arrays in Polymer Pen Lithography. *Nano Lett.* **2010**, *10*, 1335−1340.

(34) Liao, X.; Braunschweig, A. B.; Zheng, Z. J.; Mirkin, C. A. Force- and Time-Dependent Feature Size and Shape Control in Molecular Printing via Polymer-Pen Lithography. *Small* **2010**, *6*, 1082−1086.

(35) Xie, Z.; Chen, C. J.; Zhou, X. C.; Gao, T. T.; Liu, D. Q.; Miao, Q.; Zheng, Z. J. Massively Parallel Patterning of Complex 2D and 3D Functional Polymer Brushes by Polymer Pen Lithography. *ACS Appl. Mater. Interfaces* **2014**, *6*, 11955−11964.

(36) Zhou, X. C.; Wang, X. L.; Shen, Y. D.; Xie, Z.; Zheng, Z. J. Fabrication of Arbitrary Three- Dimensional Polymer Structures by Rational Control of the Spacing between Nanobrushes. *Angew. Chem., Int. Ed.* **2011**, *50*, 6506−6510.

(37) Zhou, X. C.; Liu, X. Q.; Xie, Z.; Zheng, Z. J. 3D-Patterned Polymer Brush Surfaces. *Nanoscale* **2011**, *3*, 4929−4939.

(38) Chen, C. J.; Zhou, X. C.; Xie, Z.; Gao, T. T.; Zheng, Z. J. Construction of 3D Polymer Brushes by Dip-Pen Nanodisplacement Lithography: Understanding the Molecular Displacement for Ultrafine and High-Speed Patterning. *Small* **2015**, *11*, 613−621.

(39) Huo, F. W.; Zheng, G. F.; Liao, X.; Giam, L. R.; Chai, J. A.; Chen, X. D.; Shim, W. Y.; Mirkin, C. A. Beam Pen Lithography. *Nat. Nanotechnol.* **2010**, *5*, 637−640.

DOI: 10.1021/acsami.5b01158
ACS Appl. Mater. Interfaces 2015, 7, 6991−7000

(40) Huo, F. W.; Zheng, Z. J.; Zheng, G. F.; Giam, L. R.; Zhang, H.; Mirkin, C. A. Polymer Pen Lithography. *Science* **2008**, *321*, 1658−1660.
(41) Chai, J. A.; Huo, F. W.; Zheng, Z. J.; Giam, L. R.; Shim, W.; Mirkin, C. A. Scanning Probe Block Copolymer Lithography. *Proc. Natl. Acad. Sci. U. S. A.* **2010**, *107*, 20202−20206.
(42) Cao, H.; Tegenfeldt, J. O.; Austin, R. H.; Chou, S. Y. Gradient Nanostructures for Interfacing Microfluidics and Nanofluidics. *Appl. Phys. Lett.* **2002**, *81*, 3058−3060.
(43) Turchanin, A.; Schnietz, M.; El-Desawy, M.; Solak, H. H.; David, C.; Golzhauser, A. Fabrication of Molecular Nanotemplates in Self-Assembled Monolayers by Extreme- Ultraviolet-Induced Chemical Lithography. *Small* **2007**, *3*, 2114−2119.
(44) Ok, J. G.; Kwak, M. K.; Huard, C. M.; Youn, H. S.; Guo, L. J. Photo-Roll Lithography (PRL) for Continuous and Scalable Patterning with Application in Flexible Electronics. *Adv. Mater.* **2013**, *25*, 6554−6561.
(45) Liao, X.; Brown, K. A.; Schmucker, A. L.; Liu, G.; He, S.; Shim, W.; Mirkin, C. A. Desktop Nanofabrication with Massively Multiplexed Beam Pen Lithography. *Nat. Commun.* **2013**, *4*, 2103.
(46) Park, J.; Park, J. H.; Kim, E.; Ahn, C. W.; Jang, H. I.; Rogers, J. A.; Jeon, S. Conformable Solid-Index Phase Masks Composed of High-Aspect-Ratio Micropillar Arrays and Their Application to 3D Nanopatterning. *Adv. Mater.* **2011**, *23*, 860−864.
(47) Gates, B. D.; Xu, Q.; Love, J. C.; Wolfe, D. B.; Whitesides, G. M. Unconventional Nanofabrication. *Annu. Rev. Mater. Res.* **2004**, *34*, 339−372.
(48) Lee, T. W.; Jeon, S.; Maria, J.; Zaumseil, J.; Hsu, J. W. P.; Rogers, J. A. Soft-Contact Optical Lithography Using Transparent Elastomeric Stamps: Application to Nanopatterned Organic Light-Emitting Devices. *Adv. Funct. Mater.* **2005**, *15*, 1435−1439.
(49) Bowen, A. M.; Motala, M. J.; Lucas, J. M.; Gupta, S.; Baca, A. J.; Mihi, A.; Alivisatos, A. P.; Braun, P. V.; Nuzzo, R. G. Triangular Elastomeric Stamps for Optical Applications: Near-Field Phase Shift Photolithography, 3D Proximity Field Patterning, Embossed Antireflective Coatings, and SERS Sensing. *Adv. Funct. Mater.* **2012**, *22*, 2927−2938.
(50) Rogers, J. A.; Paul, K. E.; Jackman, R. J.; Whitesides, G. M. Generating ∼90 Nanometer Features Using Near-Field Contact-Mode Photolithography with An Elastomeric Phase Mask. *J. Vac. Sci. Technol., B* **1998**, *16*, 59−68.
(51) Braunschweig, A. B.; Huo, F. W.; Mirkin, C. A. Molecular Printing. *Nat. Chem.* **2009**, *1*, 353−358.
(52) von Philipsborn, A. C.; Lang, S.; Bernard, A.; Loeschinger, J.; David, C.; Lehnert, D.; Bastmeyer, M.; Bonhoeffer, F. Microcontact Printing of Axon Guidance Molecules for Generation of Graded Patterns. *Nat. Protoc.* **2006**, *1*, 1322−1328.
(53) Qin, D.; Xia, Y. N.; Whitesides, G. M. Soft Lithography for Micro- and Nanoscale Patterning. *Nat. Protoc.* **2010**, *5*, 491−502.
(54) Han, X.; Bian, S. D.; Liang, Y.; Houk, K. N.; Braunschweig, A. B. Reactions in Elastomeric Nanoreactors Reveal the Role of Force on the Kinetics of the Huisgen Reaction on Surfaces. *J. Am. Chem. Soc.* **2014**, *136*, 10553−10556.
(55) Bian, S. D.; Scott, A. M.; Cao, Y.; Liang, Y.; Osuna, S.; Houk, K. N.; Braunschweig, A. B. Covalently Patterned Graphene Surfaces by A Force-Accelerated Diels-Alder Reaction. *J. Am. Chem. Soc.* **2013**, *135*, 9240−9243.
(56) Garcia, R.; Knoll, A. W.; Riedo, E. Advanced Scanning Probe Lithography. *Nat. Nanotechnol.* **2014**, *9*, 577−587.
(57) Kumar, G.; Tang, H. X.; Schroers, J. Nanomoulding with Amorphous Metals. *Nature* **2009**, *457*, 868−872.
(58) Xie, Z.; Shen, Y. D.; Zhou, X. C.; Yang, Y.; Tang, Q.; Miao, Q.; Su, J.; Wu, H. K.; Zheng, Z. J. Polymer Pen Lithography Using Dual-Elastomer Tip Arrays. *Small* **2012**, *8*, 2664−2669.
(59) Zhong, X.; Bailey, N. A.; Schesing, K. B.; Bian, S.; Campos, L. M.; Braunschweig, A. B. Materials for the Preparation of Polymer Pen Lithography Tip Arrays and A Comparison of Their Printing Properties. *J. Polym. Sci., Part A: Polym. Chem.* **2013**, *51*, 1533−1539.
(60) Bian, S. D.; Zieba, S. B.; Morris, W.; Han, X.; Richter, D. C.; Brown, K. A.; Mirkin, C. A.; Braunschweig, A. B. Beam Pen Lithography As A New Tool for Spatially Controlled Photochemistry, and Its Utilization in the Synthesis of Multivalent Glycan Arrays. *Chem. Sci.* **2014**, *5*, 2023−2030.
(61) Allazetta, S.; Cosson, S.; Lutolf, M. P. Programmable Microfluidic Patterning of Protein Gradients on Hydrogels. *Chem. Commun.* **2011**, *47*, 191−193.
(62) Nicosia, C.; Krabbenborg, S. O.; Chen, P.; Huskens, J. Shape-Controlled Fabrication of Micron-Scale Surface Chemical Gradients via Electrochemically Activated Copper(I) "Click" Chemistry. *J. Mater. Chem. B* **2013**, *1*, 5417−5428.

DOI: 10.1021/acsami.5b01158
ACS Appl. Mater. Interfaces 2015, 7, 6991−7000